~~CR-12~~
CR 172015

CSDL-R-2012

EFFICIENT PLACEMENT OF STRUCTURAL DYNAMICS SENSORS ON THE SPACE STATION

by

Janet A. Lepanto
G. Dudley Shepard

29 September 1987

The Charles Stark Draper Laboratory, Inc.
555 Technology Square
Cambridge, Massachusetts 02139

EFFICIENT PLACEMENT OF STRUCTURAL DYNAMICS SENSORS ON THE SPACE STATION

by

Janet A. Lepanto
G. Dudley Shepard

29 September 1987

The Charles Stark Draper Laboratory, Inc.
Cambridge, Massachusetts 01239

INTRODUCTION

System identification of the space station dynamic model will require flight data from a finite number of judiciously placed sensors on the structure. The location of these sensors on the space station will be subject to a number of constraints. One constraint is that adequate data must be obtained for each build-up flight such that the model can be identified for each phase of the assembly sequence. A second constraint is that once a given sensor is placed on the structure, it cannot be relocated. A third constraint is that only a finite complement of sensors is practical for this application. The flight data from the sensors will provide modal information for a finite number of dominant structural modes. This modal information will support a variety of applications including: design and development of the GN&C system, payloads, and model verification.

The placement of structural dynamics sensors on the space station is a particularly challenging problem because the station will not be deployed in a single mission. The build-up sequence of several assembly flights means that it is actually a series of space stations that must be instrumented, not just a final configuration. Therefore, from the first flight, the placement of the sensors must anticipate subsequent stages of build-up. The modal characteristics of a structure may change considerably as additional portions of structure are added. In particular, the shift in mode shapes must be considered when placing structural dynamics sensors. For example, a sensor that is located at the site of significant structural deflection for the first build-up flight may be at a node of vibration for some subsequent configuration. Similarly, a sensor location that is of marginal benefit on the first flight may provide data that is required to identify modal characteristics at a later stage of assembly.

Given that the build-up sequence and the final configuration for the space station are currently undetermined, our goal is to develop and demonstrate a **procedure** for sensor placement, using the assembly flights 1 through 7 of the rephased dual keel space station as an example. The procedure may then be automated in a computer program, and applied to other interim configurations, as well as to the final configuration and assembly sequence. With this in mind, note that **the sensor locations discussed in this document are relevant only to the rephased dual keel configuration** and are presented solely for purposes of illustration.

PROCEDURE FOR PLACING SENSORS

This section describes each step of the approach to placing structural dynamics sensors on the space station, subject to the assumptions and constraints described above. Additional restrictions that may be imposed by the operational capabilities of the space station were anticipated and considered to the extent possible. The specific operational and practical constraints that were taken into account are discussed below. Furthermore, this procedure assumes that the data from the sensors will support applications of system identification; the potential requirement to accommodate active vibration damping was not considered.

Finite Element Models

The first step in determining where to locate structural dynamics sensors on the space station was to analytically predict the modal characteristics of the structure. Finite element models were generated, using NASTRAN, for each of the first seven assembly flights of the rephased dual keel configuration. These flights were considered because they were the only build-up flights for which sufficient and consistent structural parameter and mass property data were available. The finite element models used an equivalent beam representation of the truss segments. All of the appendages were modeled using rigid elements to interconnect the appendage masses. The first 14 flexible mode shapes and frequencies were obtained for each of the flights. The nodes used in the finite element representation of the rephased dual keel space station are shown in Figure 1. The flexible mode frequencies for each flight are given in Table 1.

The finite element results were used to locate the parts of the structure that exhibited the most significant modal displacement at each stage of build-up. These locations, or finite element nodes, were the candidate sites for the sensors. A criterion was applied to evaluate the amount of modal displacement at each node, in each of the three translational degrees of freedom. This criterion also served to limit the number of potential sensor locations because only the locations that had sufficient displacement were retained. The only location that was not chosen according to this criterion was node 12. A sensor location was added at this node because it was intuitive to place a sensor at the midpoint of the primary structure, even though the finite element results did not recommend this location. Table 2 lists the response locations, including node 12, that are added for each build-up flight. Note that locations on appendages, as well as on the primary truss structure,

are included.

Clearly, the sensor locations given in Table 2 are too numerous to be practical for implementation on the space station. Therefore, a subset of these locations was chosen, subject to the constraint that each location be a site of significant modal displacement **for all of the build-up flights 1 through 7.** This resulted in the considerably reduced number of sensor locations added for each flight that are listed in Table 3. Again, the sensor location at node 12 is retained based on intuition. The locations of the sensors on the structure are shown in Figure 2. Note that the maximum number of sensor locations is 19, and that no sensors are added to the structure after the third build-up flight. This is due to the fact that after flight 3, the primary structure of the station is in place and subsequent build-up flights add only localized masses such as modules and payloads. Although the addition of these masses does change the mode frequencies and mode shapes of the structure, the procedure predicted that the sensors that are in place as of flight 3 will provide sufficient data for system identification of modal characteristics through flight 7.

Modal Frequency Response Analysis

The sensor locations that are listed in Table 3 were derived solely from finite element predictions of the modal characteristics for each assembly configuration. A modal frequency response analysis was implemented for each build-up flight, using NASTRAN, to evaluate the modal participation at these sensor locations and to determine whether closely spaced modes could be distinguished from each other. This analysis provided the frequency response functions for the three translational degrees of freedom at each sensor location due to inputs at a particular location along two different axes. The first input was a unit sinusoid along the x-axis of the space station, and the second input was a unit sinusoid along the z-axis. Note that an input along the y-axis was not used since the finite element analysis indicated that few modes have significant axial components along the main truss of the space station. The input excitations were applied at the location of the RCS pod on the starboard transverse boom, which is at node 104 in Figure 2. This RCS pod is deployed on the first build-up flight and will therefore be available as an excitation source throughout the assembly sequence.

The acceleration frequency response to these inputs was generated at each sensor location for each translational degree of freedom. An example of the modal frequency response plots that were obtained is shown in Figure 3. The acceleration response was used rather than the displacement response because the amplitude of the displacement response decreases rapidly with increasing frequency. Furthermore, although the first priority of system identification for the space station is

to obtain modal frequencies and damping, if mode shape information is also desired, it is more easily derived from accelerometer data than from strain gauge data. Therefore, it is assumed that a triaxial accelerometer will be mounted at each of the sensor locations to provide flight data for system identification. The frequency response plots were studied for each build-up flight to determine which structural frequencies will be observed by the accelerometers at the candidate locations. The results are tabulated for all seven flights at two levels of acceleration. The first tabulation of observed frequencies requires that the amplitude of the acceleration be greater than or equal to 0.1 inches/sec^2; the second tabulation requires that the amplitude of the acceleration be greater than or equal to 0.01 inches/sec^2. Note that both of these acceleration levels are based on a unit sinusoid force and can be scaled to actual acceleration levels when the real input force is defined. Table 4 shows the modes that were not observed at each of the sensor locations on a flight by flight basis, for both acceleration levels.

RESULTS OF MODAL FREQUENCY RESPONSE ANALYSIS

The goal of the modal frequency response analysis was to verify that sensors placed at the candidate locations on the space station would provide adequate data for system identification throughout the assembly sequence. However, as the procedure evolved, it became apparent that the results could provide a much broader insight into the problem of instrumenting a structure like the space station. This section first discusses how successful the procedure was in identifying appropriate sensor locations, and then considers some additional aspects of the problem that surfaced as the procedure was developed. These aspects include: unobserved modes, dominant structural modes, and trade-offs in sensor placement.

Evaluation of Sensor Locations

The tabulations of the observed modes based on the modal frequency response analysis indicate that the procedure was successful in choosing viable locations for structural dynamics sensors. Table 5 summarizes the modes that were "missing" (i.e. not observed at **any** sensor location) at each of the acceleration levels defined in the preceding section. These results indicate that if the second acceleration level is used as the criterion for judging the observability of frequencies, then the first 14 flexible mode frequencies will be observable throughout the assembly sequence. If the first acceleration level is used as the criterion for observability, then for several flights some modes will not be observed.

It is interesting to note that the sensor located at finite element node 12 (which was not chosen by the procedure as a viable location), provides very little data for any mode of any build-up configuration after flight 4. Furthermore, the few modes that are observed at this location are observed at nearly all of the other sensor location so that, at best, a sensor at node 12 will provide redundant information. This reinforces the argument that sensor locations for a structure as complicated as the space staion cannot be chosen by intuition or symmetry.

Unobserved Modes

It is important to understand why a given mode is unobserved at a particular sensor location. One possibilty is that the mode is a local mode. A local mode occurs when the modal acceleration is localized to one part of the structure, such as an appendage. In this case, a sensor is unlikely to detect the mode unless the sensor is placed at, or very near, the site of the local mode. Therefore, a local mode will be observed by at most one or two sensors. A second possible explanation of an unobserved mode is that the mode is inefficiently excited by the test input. In this case, the modal acceleration will be small everywhere on the structure and therefore it is unlikely to be detected at any sensor location.

The difference between local modes and inefficiently excited modes can be seen in Table 4. For example, consider mode 10 and mode 15 of flight 6 in the assembly sequence. Mode 15 is unobserved at all of the sensor locations except at finite element node 102, which suggests that this is a local mode. Not surprisingly, Figure 1 shows that 102 is located at the tip of an appendage. Mode 10 is not observed at any of the sensor locations, which is characteristic of an inefficiently excited mode. When the mode shape for mode 10 is examined in Figure 4, it can be seen that the location of the input, at finite element node 104, is actually at a modal node, which results in the mode being inefficiently excited.

The concept of inefficiently excited modes is a significant aspect of the system identification problem for the space station. A mode that is inefficiently excited by the test input is not likely to be identified from the on-orbit test data. This does not mean that the mode is not present, but it does imply that no experimental knowledge of the mode will be available from on-orbit tests. Furthermore, it is possible that a mode which is inefficiently excited by the test input will be excited by transients from operational activities such as docking or maneuvers of the mobile remote manipulator system (MRMS). The potential for exciting an unidentified mode could degrade the performance of the GN&C system and could also prove unacceptable to the space station payload users. Therefore, if it is determined a priori that a particular mode will be inefficiently excited by the

test input, and if there is a need to verify the characteristics of that mode, then an additional test input must be designed to facilitate identification of the mode.

Dominant Structural Modes

The 19 sensor locations in Figure 2 were chosen assuming that there is a requirement to identify the first 14 flexible modes of the space station for each of the 7 build-up flights. However, it is likely that the structural response of the space station will be dominated by a subset of these modes for a wide range of on-orbit operations and activities. The modal frequency response analysis that was used to verify the sensor locations can also be implemented to predict the dominant structural modes for each build-up flight. This assumes, of course, that detailed models of realistic excitations will be available to use as inputs. For example, to predict which modes will be excited by operational use of the RCS jets, it will be necessary to know the pulse length, thrust limit, and firing sequence of the jets. Similarly, dominant structural modes can be predicted from the structural response to other space station operations, such as docking, MRMS activity, and orbit maintenance.

The results of the analysis to determine the dominant modes will provide an additional set of criteria by which to evaluate the candidate sensor locations. For example, some of the sensor locations may not be necessary because the modes that do not dominate the response of the structure under operational conditions will be eliminated from the system identification problem. Alternatively, additional sensor locations may be required to provide redundant mode shape and frequency data for particularly critical modes. The prediction of dominant structural modes will also indicate whether additional test inputs are warranted to identify the inefficiently excited modes. Unless it is demonstrated that an inefficiently excited mode is a dominant mode in the response of the structure, it will not be necessary to verify the characteristics of that mode. This will help to limit the number of on-orbit tests that are required to support the system identification of the space station.

Trade-offs in Sensor Placement

Practical considerations may preclude the use of some of the sensor locations that are given in Table 3. Restrictions imposed by the data management system may limit the number of sensors from which data can be processed, and some locations may be reserved for payloads that cannot accommodate a sensor package. The tabulations of the unobserved modes at each sensor location

for each build-up flight (cf. Table 4) can be used to evaluate the trade-offs associated with eliminating sensor locations from the structure. One trade-off is between the number of sensor locations and the modal characteristics that can be identified from the sensor data. As the number of available sensors decreases, system identification will be restricted to mode frequency and damping since these parameters, unlike mode shape, can be identified even if data for each mode is only obtained at one or two locations. As the number of available sensors decreases further, even frequency and damping characteristics will be unidentifiable for some modes.

Another trade-off is between the number of sensors and the amount of redundancy that is available. The issue of redundancy is not addressed directly in this study. However, if there is a high priority associated with the identification of certain dominant modes, then data from which to identify these modes must be available from more than one sensor.

The information in Table 4 can also be used to assess the relative value of each sensor location. Some of the sensor locations will provide data for several modes that characterize each build-up configuration. These locations are particularly good choices to support system identification. Other locations will provide data for only one or two local modes, and therefore do not appear to be good choices if the number of available sensor locations is limited. However, before these locations are eliminated, it must be determined that the local modes that are observed are not of interest.

SUMMARY AND CONCLUSIONS

This procedure approaches the problem of placing structural dynamics sensors on the space station from an engineering, as opposed to a mathematical, point of view. Given a structure such as the space station, there are several reasons why an engineering approach to sensor placement is appropriate. First, many of the constraints that will be imposed by space station operations can be anticipated even though the final configuration for the system is not yet determined. These constraints must be considered in the sensor placement problem because they will restrict the number of sensors that can be used and also where these sensors can be located. For example, the capacity of the data management system will limit the number of sensors from which data can be processed. Another justification for an engineering approach to sensor placement arises from the fact that the space station will be deployed in a series of build-up flights. Sensors will be placed on each successive segment of the structure to support system identification of each build-up configuration. Since it will be impractical to relocate sensors on the structure after deployment, all of the sensors must be placed on the space station such that each sensor provides useful data

throughtout the assembly sequence.

In addition to locating a finite number of sensors, the procedure addresses the issues of unobserved structural modes, dominant structural modes, and the trade-offs involved in sensor placement for space station. The procedure utilizes a simple, yet effective, format for organizing structural dynamics data (cf. Table 4). This format facilitates an evaluation of the trade-offs between the number of sensors and the degree of redundancy, and between the number of sensors and the modal characteristics that can be identified from flight data. The format is also useful in distinguishing between local modes and modes that are inefficiently excited by the test input.

This procedure for sensor placement will be applied to revised, and potentially more detailed, finite element models of the space station configuration and assembly sequence. Before this can be done, however, it will be necessary to automate several steps of the procedure in a computer program. For example, any step where a quantitative criterion is applied can be accomplished more easily and less tediously by a computer than by hand.

Sensor placement is but one aspect of the system identification problem for a large, complicated structure such as the space station. Moreover, the number of sensors and where they are located on the structure is highly dependent on the requirements for system performance, the capacity of the data management system, the design of the test inputs, and the modal characteristics that are to be identified. Given these constraints and considerations, the placement of sensors on the structure is not intuitive and the sensors are not distributed uniformly or symmetrically. The procedure for sensor placement discussed above incorporates these constraints to select a finite complement of structural dynamics sensors which will provide adequate data for system identification.

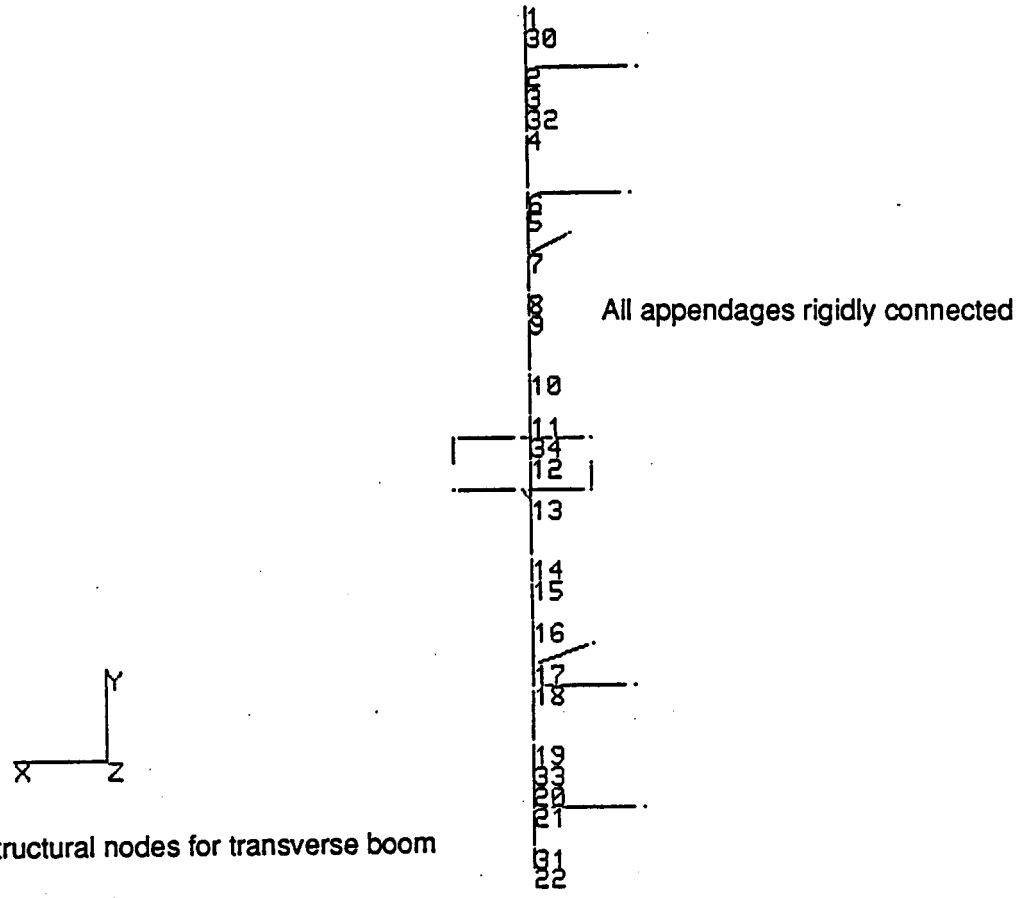

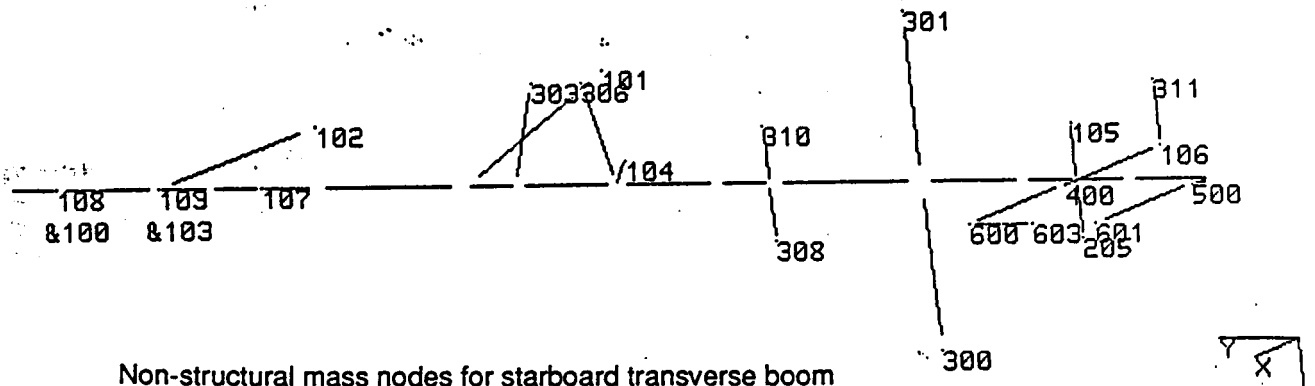

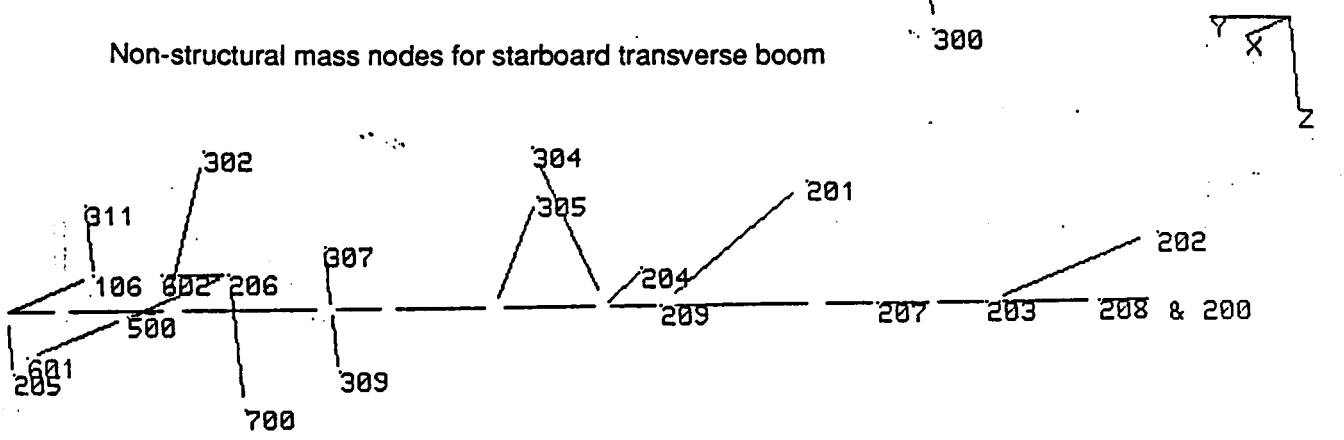

FIGURE 1. Finite element representation of rephased dual keel showing node locations

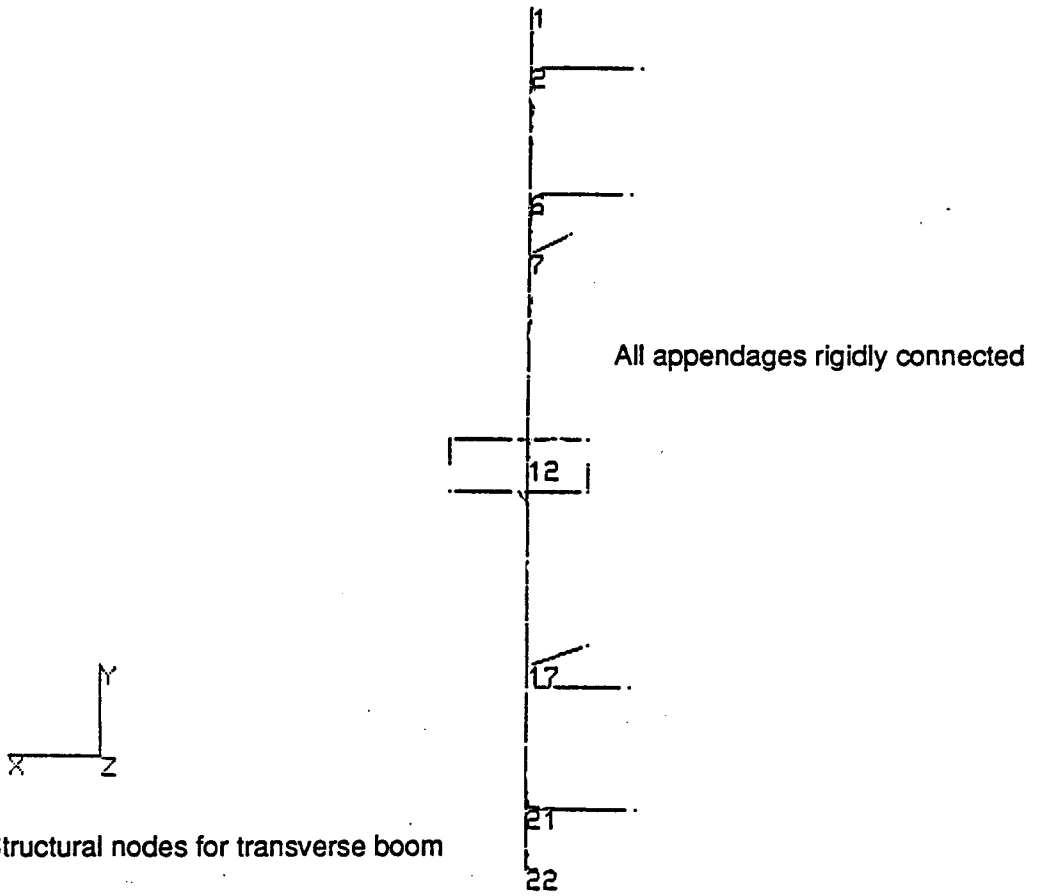

Structural nodes for transverse boom

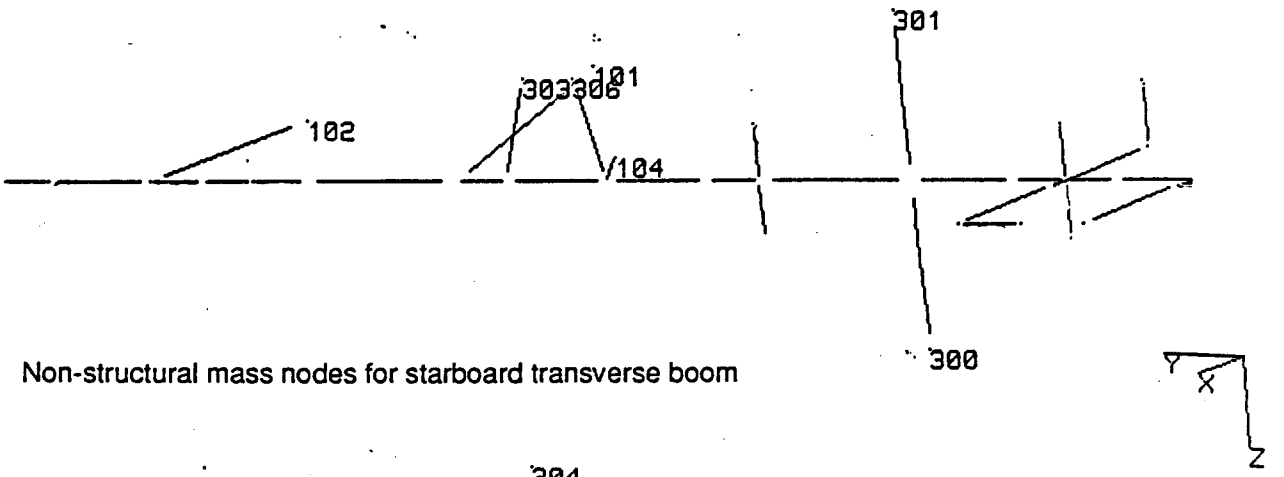

Non-structural mass nodes for starboard transverse boom

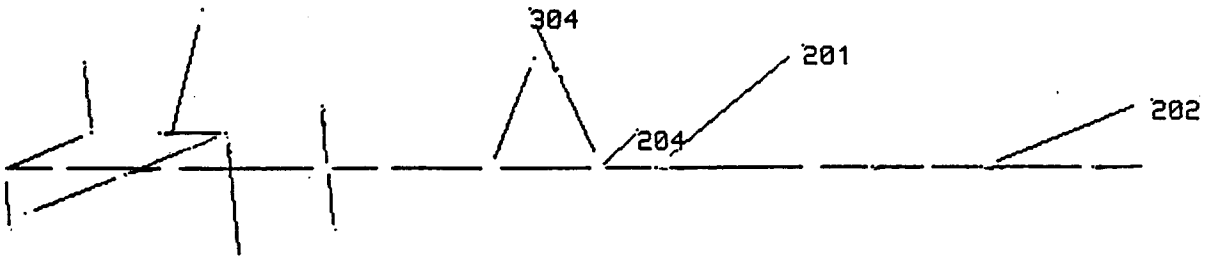

Non-structural mass nodes for port transverse boom

FIGURE 2. Reduced number of candidate sensor locations on the structure

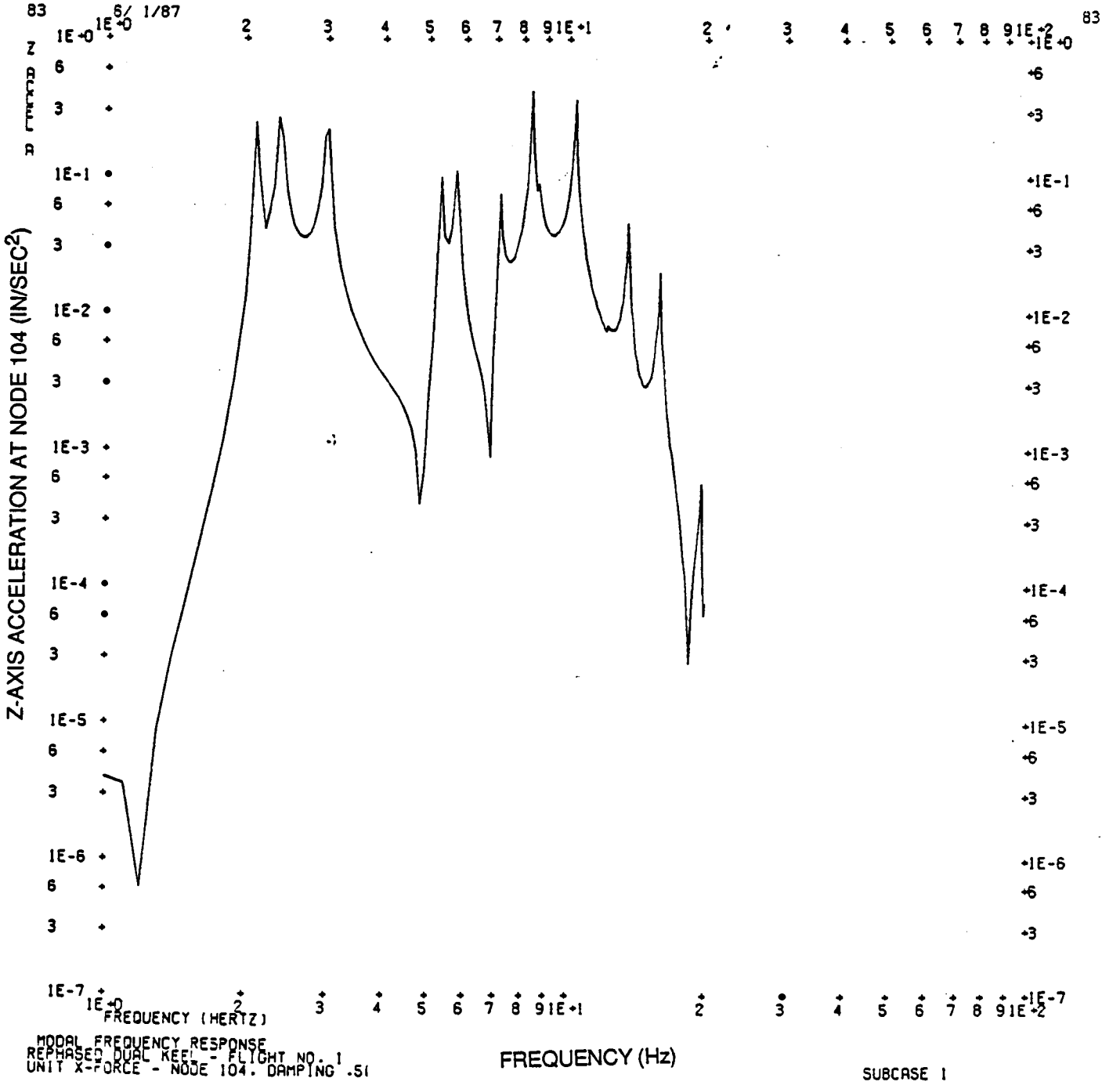

FIGURE 3. Example of modal frequency response plot

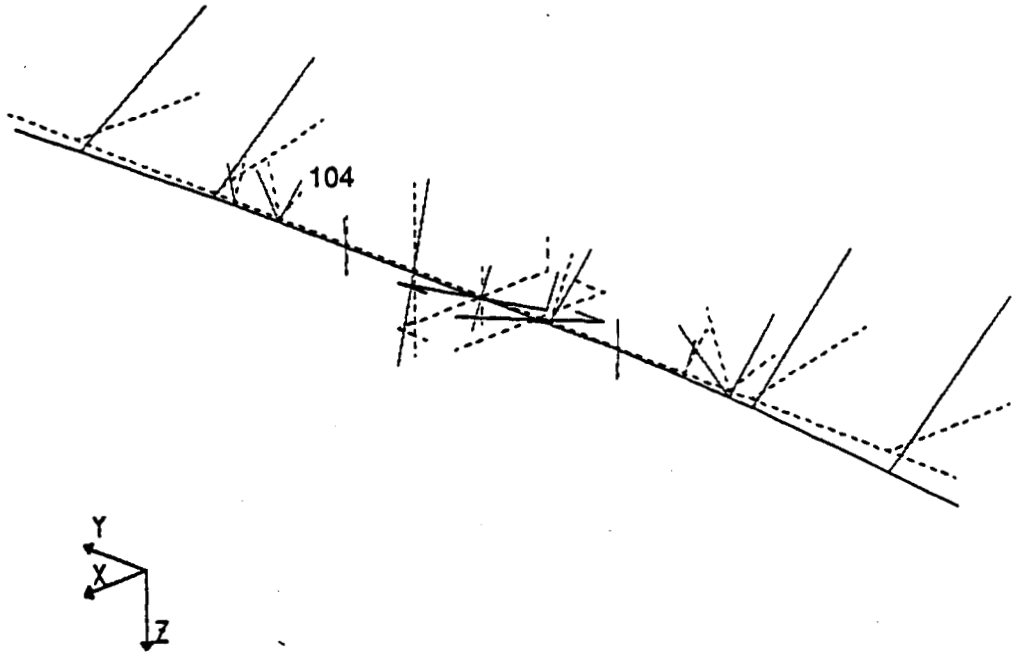

FIGURE 4. Mode shape for mode 10, Flight 6

	MODE													
FLIGHT	1	2	3	4	5	6	7	8	9	10	11	12	13	14
1	2.09	2.16	2.37	2.98	5.29	5.73	7.10	8.30	8.56	10.29	12.15	13.44	15.79	19.56
2	0.61	0.62	0.74	2.05	2.14	2.19	2.35	2.69	3.50	3.83	4.52	4.90	5.50	5.88
3	0.57	0.58	0.73	1.50	1.83	1.91	2.29	2.45	3.22	3.33	3.45	4.38	4.66	4.81
4	0.53	0.54	0.73	1.15	1.73	1.82	2.26	2.43	3.02	3.22	3.29	3.80	4.36	4.37
5	0.51	0.52	0.73	1.09	1.58	1.71	2.15	2.27	2.41	2.60	3.22	3.77	4.18	4.26
6	0.51	0.52	0.72	1.02	1.50	1.70	1.85	2.26	2.39	2.85	3.19	3.69	3.96	4.24
7	0.50	0.51	0.71	0.95	1.37	1.50	1.61	2.24	2.34	2.65	2.98	3.69	3.91	4.14

TABLE 1. Frequencies of flexible modes for each build-up flight (Hz)

FLIGHT	SENSOR LOCATIONS ADDED
1	1,2,5,6,7,30,100,101,102,103,104,108,109
2	12,17,18,21,22,31,200,201,202,203,204,208,209
3	300,301,303,304,306
4	No locations added
5	No locations added
6	No locations added
7	No locations added

TABLE 2. Candidate sensor locations added for each build-up flight

FLIGHT	SENSOR LOCATIONS ADDED
1	1,2,6,7,101,102,104
2	12,17,21,22,201,202,204
3	300,301,303,304,306
4	No locations added
5	No locations added
6	No locations added
7	No locations added

TABLE 3. Reduced list of sensor locations added for each build-up flight

SENSOR	MODE													
	7	8	9	10	11	12	13	14	15	16	17	18	19	20
1											|			
2		|		|							|			
6														
7														
102											|			
101											|			
104														

TABLE 4a. Unobserved modes at each sensor for Flight 1

NOTE: In Table 4 a-g: "|" indicates an unobserved mode for acceleration level > 0.1 in/sec^2

"+" indicates an unobserved mode for acceleration level > 0.01 in/sec^2

SENSOR	MODE													
	7	8	9	10	11	12	13	14	15	16	17	18	19	20
1	|	|		+							|	|		
2	|	|	|	+			|	+			|	|	|	
6	+	+	|	+							|	|		
7	+	+	|	+							|	+	|	
12	|	|	+	+			|	|			+	+	|	
102	|	|		+							|	|		
101	|	|		+							|	|		
104	+	+	|	+							|	+		
201	|	|		|						|	|	|		
202	|	|		+							|	|		
22	|	|		|						|	|		
21	|	|	|	+			|	|			|	|	|	
17	+	+	|	+							|	|	|	
204	|	|		+							|	|		

TABLE 4b. Unobserved modes at each sensor for Flight 2

SENSOR	MODE													
	7	8	9	10	11	12	13	14	15	16	17	18	19	20
1	|	|		|				|				|	|	
2	|	|	|	|			|	|	|	|	|	|	|	|
6	+	+	|	|			|	|				|	|	
7	+	+	|	|			|	|				|	|	
12	|	|	+	|			|	|				|		|
102	|	|										|	|	
101	|	|										|	|	
104	+	+	+	|				|				|		
201	|	|										|		
202	|	|										|		
22	|	|		|			|	|				|		
21	|	|		|			|	|	|	|	|		|
17	+	+	|	|			|	|				|		
204	|	|		|				|				|	|	
303	|	|		|			|					|	|	|
300	|	|	|				|	|				|		
301	|	|	|				|	|				|		
304	|	|		|								|		
306	+	+		|			|	|				|		|

TABLE 4c. Unobserved modes at each sensor for Flight 3

SENSOR	MODE													
	7	8	9	10	11	12	13	14	15	16	17	18	19	20
1			|	|				|			|		
2			|	|			|	|	|	|	|		
6	|	|	|	+			|	|				|		
7	|	|	|	|				|				+		
12	|	|	+	|	|	|	|	|		|	|	|		
102												|		
101	|	|								+				
104	|	|		|				|					
201	|	|						|		|			
202														
22				|				|					
21				|			|	|	|	|	|	|	|	|
17	|	|	|	+				|					
204	|	|		|				|					
303	|	|		|				|				|		
300	|	|					|	|					
301	|	|					|	|					
304	|	|		|				|					
306	|	|		|				|					

TABLE 4d. Unobserved modes at each sensor for Flight 4

SENSOR	MODE													
	7	8	9	10	11	12	13	14	15	16	17	18	19	20
1			|	|			|	|	|			|		
2			|	|			|	|	+		|	+	|	|
6	|	|	|	|			|	|	|			|		
7	|	|	|	+			|	|	|			|		
12	|	|	+	+	|	|	|	|	+		|	|	|	|
102									|			|		
101				|			|		|					
104	|	|		+					+					
201				|					|		|	|		
202				|					|			|		
22				|			|		+			|		
21			|	|				|	+			|		
17	|	|	|	+			|	|	+			|		
204	|	|		|			|		|			|		
303	|	|		|			|	|	|			|		
300	|	|	|	|					|					
301	|	|	|	|				|	|					
304	|	|		|			|		|			|		
306	|	|		|			|	|	|					

TABLE 4e. Unobserved modes at each sensor for Flight 5

SENSOR	MODE													
	7	8	9	10	11	12	13	14	15	16	17	18	19	20
1				|			|		+			|		|
2				|			|	|	+		|	+	|	|
6	|	|	|	+			|	|	|			+		|
7	|	|	|	|			|	|	|			+		|
12	|	|	+	+	|	|	+	|	+			+	|	+
102				|									|		
101	|	|		|			|		|					|
104	|	|		|			|		+					|
201	|	|		|			|		|		|	|		|
202					|					|			|		|
22					|			|		+			|		|
21					|			|	|	+		|	+	|	|
17	|	|	|	+			|		|			|		|
204	|	|		|			|		|			|		|
303	|	|		|			|		|			|		|
300	|	|		|				|	|					|
301	|	|		|			|	|	|					|
304	|	|		|			|		|			|		|
306	|	|		|			+	|	|						|

TABLE 4f. Unobserved modes at each sensor for Flight 6

SENSOR	MODE													
	7	8	9	10	11	12	13	14	15	16	17	18	19	20
1				|					|			|		
2				|	|	|		|	|		|	+		|
6			|	+	|	|			|			|		
7	|	|	|	+	|				|			|		
12	|	|	|	+	+	|	|	|	+		|	+	|	+
102												|		
101						|								
104	|	|		|					|					
201						|						|		|
202												|		
22			|	|					|			|		|
21			|	|		|		|	|		|	+	|	|
17			|	|	|	|			|			|		|
204	|	|			|	|			|			|		|
303				|					|			|		|
300	|	|		|					|					|
301	|	|		|	|				|					|
304	|	|			|	|			|			|		|
306	|	|		|					|					|

TABLE 4g. Unobserved modes at each sensor for Flight 7

FLIGHT	MISSING MODES	
	Acceleration level >0.1 in/sec^2	Acceleration level >0.01 in/sec^2
1	None	None
2	7,8,10,17,18	None
3	7,8,18	None
4	None	None
5	15	None
6	10	None
7	None	None

TABLE 5. Summary of unobserved modes at each acceleration level